

Branch content of metallocene polyethylene

Ramnath Ramachandran, Gregory Beaucage* and Amit Kulkarni
*Department of Chemical and Materials Engineering, University of Cincinnati,
Cincinnati, Ohio 45221, USA*

Douglas McFaddin, Jean Merrick-Mack and Vassilios Galiatsatos
*Equistar Chemicals, LP, a LyondellBasell Company, Cincinnati Technology Center,
11530 Northlake Drive, Cincinnati, Ohio 45249, USA*

Small-angle neutron scattering is used to investigate the structure and long-chain branch (LCB) content of metallocene catalyzed polyethylene (PE). A novel scaling approach is applied to determine the mole fraction branch content (ϕ_{br}) of LCBs in PE. The approach also provides the average number of branch sites per chain (n_{br}), average number of branch sites per minimum path ($n_{br,p}$), average branch length (z_{br}) and number of inner segments (n_i), giving insight into the chain architecture. The approach elucidates the relationship between the structure and rheological properties of branched PE.

PACS numbers: 61.25.H-, 61.05.fg, 61.41.+e, 83.80.Rs

Structural branching is known to occur in a variety of materials such as polymers and ceramic aggregates [1, 2]. Owing to the influence of branching on the physical and chemical properties of these materials, a universal technique to quantify the branch content has been long sought. A new scaling model [3] has recently been developed to quantify branch content in such ramified structures. The scaling model has been employed successfully to study ceramic aggregates [3] and to describe the folded and unfolded state in proteins and RNA [4]. This model can be used to quantify long-chain

* Corresponding author

branching in polymers as well. Long-chain branching has significant influence on the physical properties displayed by a polymer. The presence of long-chain branches (LCBs) considerably affects the structure and consequently the rheological properties and processability of polymers [5-8]. Hence, an efficient and comprehensive method to quantify long-chain branch (LCB) content in polymers has been desired for many years. Various techniques have been utilized to determine LCB content in branched polymers [9-13]. Existing techniques are ineffective in characterizing low levels of LCB and have problems in distinguishing between short and long-chain branches. The most sensitive, rheological methods tend to be semi-empirical and qualitative in nature [13]. NMR is an effective technique to determine the total number of branch sites (β) in a few polymers. In this letter, a scaling model [3] is applied to small angle neutron scattering (SANS) data obtained from dilute solutions of metallocene polyethylene samples, to quantify the LCB content in polymers previously studied by NMR and rheology [11, 12].

A polyethylene (PE) chain can be considered to exhibit two structural levels, the overall radius of gyration R_g with mass fractal dimension d_f and the substructural rod-like persistence length l_p or Kuhn length $l_k=2l_p$ [14]. These features can be observed in a small angle scattering pattern and can be determined through the application of local scattering laws and mass-fractal power laws under the Rayleigh-Gans approximation. Local scattering laws such as Guinier's law and power laws describe these levels. Guinier's law is given by [15],

$$I(q) = G \exp\left(\frac{-q^2 R_g^2}{3}\right) \quad (1)$$

where $I(q)$ is the scattered intensity, scattering vector $q = 4\pi\sin(\theta/2)/\lambda$, θ is the scattering angle, λ is the wavelength of radiation, R_g is the coil radius of gyration, G is defined as $N_p n_p^2$ where N_p is the number of polymer coils in given volume and n_p is the contrast factor equal to the excess number of electrons for x-ray scattering. The mass-fractal power law is another local scattering law.

$$I(q) = B_f q^{-d_f} \text{ for } 1 \leq d_f < 3. \quad (2)$$

It describes a mass-fractal object of dimension d_f , where B_f is the power-law prefactor. Together, they give an account of local features like size (R_g and l_p) and surface/mass scaling [3, 16, 17]. Beaucage [3,16-19] has described a scaling model which can be employed to quantify branch content in polymers. A branched polymer chain of size $R_{g,2}$ is considered to be composed of z freely jointed Kuhn steps each of size l_k [18, 19] as shown in Fig. 1a. The structure of the branched polymer can further be decomposed into a minimum path p (number of Kuhn steps in the minimum path) through the structure as shown in Fig. 1a. p is an average traversing path through the chain structure. A scaling relationship can be proposed between z and p [3],

$$z = p^c = s^{d_{\min}} \quad (3)$$

where c is the connectivity dimension assuming the scaling prefactor to be one.

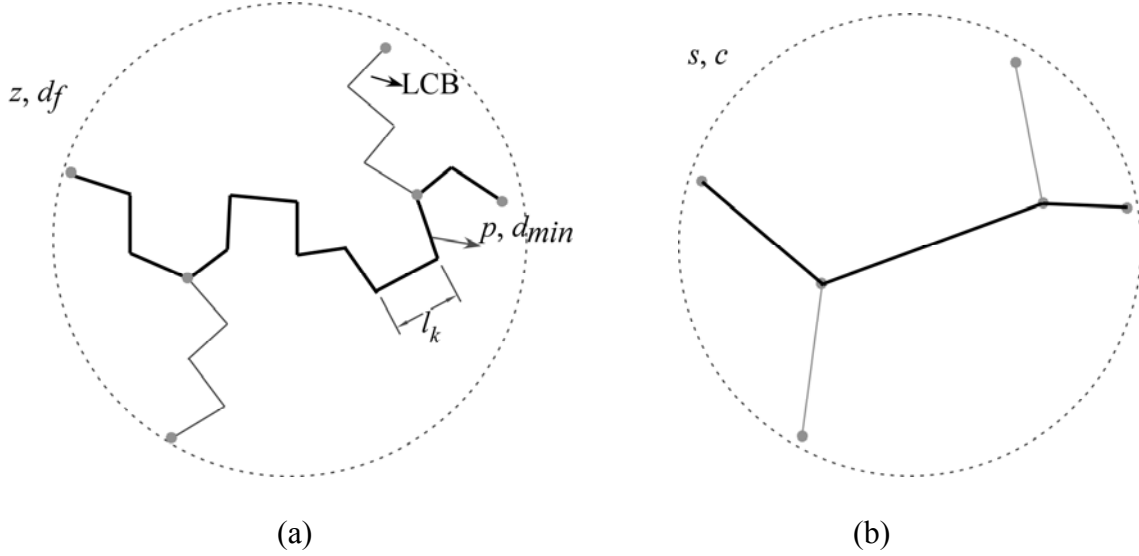


FIG. 1. (a) Schematic of a branched polymer: The polymer is composed of Kuhn steps of length l_k . The dark lines represent the minimum path p of dimension d_{min} . The lighter lines represent the long-chain branches (b) Connective path represented by straight lines connecting branch points and free ends (grey dots), of total size s and connectivity dimension c .

The minimum path p , is a mass-fractal of dimension d_{min} and size $r \sim p^{1/d_{min}}$ while the total chain of z Kuhn steps has a dimension $d_f \geq d_{min}$ and the same size $r \sim z^{1/d_f}$. A parameter s (Eq. (3)) can also be defined using d_{min} that reflects the number of steps required to connect all branch points and end points in the polymer structure by straight lines (size $r \sim s^{1/c}$). Substituting $p \sim r^{d_{min}}$ in Eq. (3) and comparing with $z \sim r^{d_f}$ yields $d_f = cd_{min}$, which shows that the chain scaling (d_f, z) can be decomposed into contributions from chain tortuosity (d_{min}, p) and chain connectivity (c, s). For a linear polymer chain $d_{min} = d_f$ and $c = 1$. On the other hand, for a completely branched object like a sphere or a disk, where a linear minimum path can be traversed, $d_f = c$ and $d_{min} = 1$. The minimum path dimension, d_{min} , and connectivity dimension c represent different features of the branched chain. While c increases with increased branching or connectivity, d_{min} increases with tortuosity in the chain, driven by the thermodynamics in a dilute polymer

solution. That is, for a linear chain in good solvent $d_{min} = 5/3$ and $c = 1$. For a branched chain, $1 < c \leq d_f$ and $1 \leq d_{min} \leq 5/3$. d_{min} deviates from $5/3$ because the minimum path can find shortcuts through the branched structure. From the scaling model, the mole fraction branches (ϕ_{br}) is given by [3],

$$\phi_{br} = \frac{z-p}{z} = 1 - z^{\frac{1}{c}-1} \quad (4)$$

Eqs.(1) and (2) can be used to calculate d_f , c , p and s . d_{min} can be calculated from [3]

$$d_{min} = \frac{B_f R_{g,2}^{d_f}}{C_p \Gamma\left(\frac{d_f}{2}\right) G} \quad (5)$$

where C_p is the polydispersity factor [19, 20] and Γ is the gamma function.

For a long-chain branched polymer, as shown Fig. 1a, branch sites occur along the minimum path through the structure. The minimum path is composed of segments, defined by the average number of Kuhn steps between branch points or chain ends, $n_{k,s}$. The average number of segments per minimum path is given by $n_{s,p}$. The end-to-end distance of the minimum path, r , in units of number of Kuhn steps can then be given by,

$$r = n_{s,p} \left(\frac{p}{n_{s,p}} \right)^{3/5} \quad (6)$$

For a branched polymer chain, r can also be described in terms of p (Fig. 1a) as $r = p^{1/d_{min}}$.

Equating with Eq. (6), we obtain the following relationship,

$$n_{s,p} = \left[p^{\left(\frac{1}{d_{min}} - \frac{3}{5} \right)} \right]^{5/2} \quad (7)$$

The number of branch sites per minimum path is then given by $n_{br,p} = n_{s,p} - 1$.

The average number of Kuhn steps in a segment, $n_{k,s}$, can be described by,

$$n_{k,s} = \frac{p}{n_{br,p} + 1} = \frac{z}{2n_{br} + 1} \quad (8)$$

where n_{br} is the number of branch sites per chain, $n_{br,p}+1$ is the number of segments in the minimum path and $2n_{br}+1$ is the total number of segments in the polymer.

From Eq. (3), we can rewrite Eq. (8) as,

$$n_{br} = \left(\frac{z \left(\frac{5}{2d_f} - \frac{3}{2c} \right)^{+(1-c)} - 1}{2} \right) \quad (9)$$

This quantity is equivalent to the average number of branches per chain, β , obtained from NMR [3, 13, 21]. The mole fraction branch content, ϕ_{br} , combined with n_{br} can be used to estimate a new quantity, the average branch length (z_{br}), from the following relationship,

$$z_{br} = \frac{z \phi_{br} M_{Kuhn}}{n_{br}} \quad (10)$$

where M_{Kuhn} is the mass of one Kuhn step as determined from the Kuhn length, $l_k = 2l_p$, of a polyethylene sample [19], which is $l_k \times 13.4$ g/mole/Å. The quantity n_{br} obtained from this analysis is compared with β obtained from NMR [21] in Fig. 2a.

We used metallocene catalyzed model branched polyethylene chains with low degrees of structural branching and narrow molecular weight distribution (Table. I).

TABLE I. Characterization of long-chain branching in DOW HDB samples.

Sample	LCB/ 10^3 ¹³ C NMR ^a	M_n (g/mole) ^a	PDI (M_w/M_n) ^a	β	n_{br}	$n_{br,p}$	d_f	c	ϕ_{br}	l_p (Å)	z_{br} (g/mole)
HDB-1	0.026	39,300	1.98	0.073	0.080	0.047	1.70	1.03	0.10	6.5	12,700
HDB-2	0.037	41,500	1.93	0.110	0.115	0.053	1.71	1.04	0.14	6.7	17,400
HDB-3	0.042	41,200	1.99	0.124	0.144	0.065	1.73	1.05	0.17	6.6	16,500
HDB-4	0.080	39,200	2.14	0.224	0.262	0.090	1.78	1.08	0.28	6.9	18,600

^aReference [21].

These samples have been extensively studied and characterized in the literature [11, 12, 21]. SANS was performed on dilute solutions of these model polyethylenes in deuterated p-xylene which is a good solvent for polyethylene at 125° C. Standard 2 mm path length quartz cells (banjo cells) were used. Deuterated p-xylene was purchased from Sigma-Aldrich. The samples were equilibrated at 125 °C for 3 hours prior to the measurements to ensure complete dissolution of the solute. 1 wt. % solution was used, well below the overlap concentration as described by Murase et al. [22] and as verified by superimposition of normalized data from 0.25 wt. %, 0.5 wt. % and 1 wt. % for the same polymer solution. SANS experiments were carried out at the Intense Pulsed Neutron Source (IPNS), Argonne National Laboratory, Argonne and National Institute of Standards and Technology (NIST) Center for Neutron Research (NCNR), Gaithersburg, NG-7 SANS. Standard data correction procedures for transmission and incoherent scattering along with secondary standards were used to obtain $I(q)$ vs. q in absolute units. Experimental runs took approximately 4 hours per sample at IPNS and 2 hours at NIST.

SANS data is fit to the Unified Function [16-19] followed by the application of the scaling model [3]. Table. I lists the sample names, NMR branch content in terms of number of long-chain branches per 1000 carbon atoms [21], LCB/10³C, number average molecular weight [21], M_n , polydispersity index (M_w/M_n) [21], PDI and average number of branch sites per chain, β , from NMR [21]. The NMR branch content, in terms of number of long-chain branches per 1000 carbon atoms, is converted to average number of branch sites per chain, β , using the relationship [21],

$$\beta = \frac{(\#LCB/1000)_{NMR} M_n}{14,000} \quad (11)$$

where, M_n is the number average molecular weight of the polyethylene, and 14,000 g/mole refers to the molar mass of 1000 backbone carbons. Table. I further lists the quantities measured from SANS including number of branch sites per chain, n_{br} , number of branch sites per minimum path, $n_{br,p}$, from Eqs. (7) to (9), mass-fractal dimension, d_f , connectivity dimension, c , mole-fraction branches from Eq. (4), ϕ_{br} , persistence length [19], l_p , and average branch length from Eq. (10), z_{br} .

Fig. 2a plots n_{br} calculated from Eq. (9) against β from Ref. [21] with good agreement. Fig. 2b plots $n_{br,p}$ against n_{br} . For a comb or 3 arm star structure (top inset, Fig. 2b), with no branch-on-branch structure, it is expected that $n_{br,p} = n_{br}$. For a more complex structure displaying branch-on-branch topology, $n_{br,p} < n_{br}$. While n_{br} measures every branch point in a polymer chain, $n_{br,p}$ reflects the number of branch points in the minimum path. Although we observe a monotonic relationship in the plot, $n_{br,p}$ is lower than n_{br} for the HDB samples. This implies the presence of branch-on-branch architecture in these samples. The plot of $n_{br,p}$ versus n_{br} in Fig. 2b, shows a stronger deviation at higher branch content. The $n_{br,p}$ value plateaus at about 0.1 indicating that the minimum path branch content reaches a constant value while additional branches are added through branch-on-branch structures. That is, the system consists of a few hyperbranched chains in a majority of linear chains at high branch content, rather than a uniform distribution of branching.

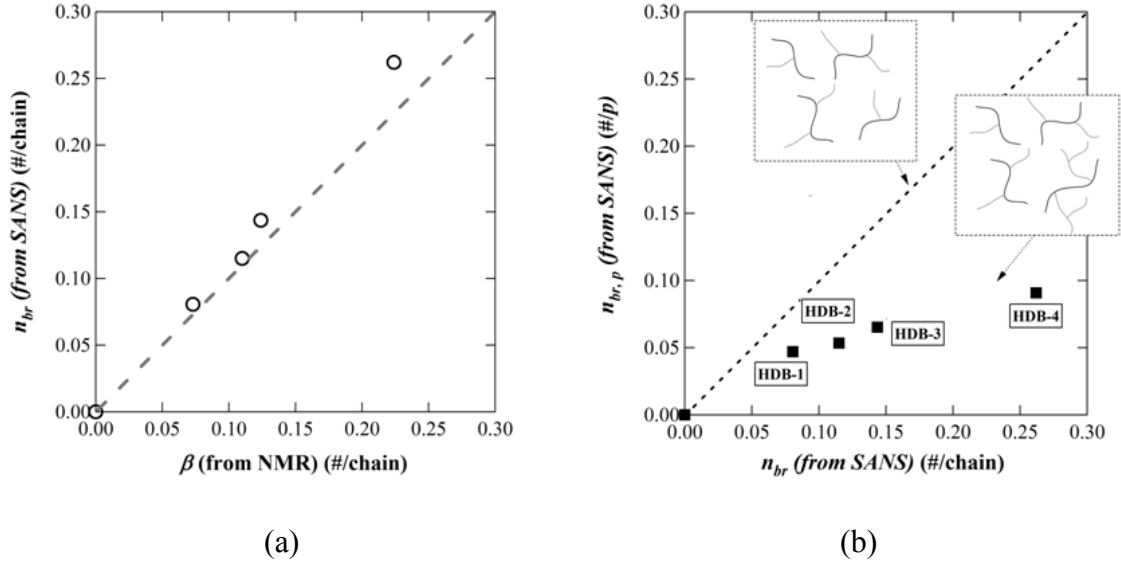


FIG. 2. (a) Plot of number of branch sites per chain, n_{br} , calculated from Eq. (9) against average number of branches per chain, β , from NMR [21]. The dashed line represents $n_{br} = \beta$. (b) Plot of number of branch sites per minimum path, $n_{br,p}$, against n_{br} calculated from Eq. (9). The dotted line represents $n_{br} = n_{br,p}$.

As mentioned earlier, the average branch length, z_{br} , can have significant impact in understanding the rheological behavior of long-chain branched polymers. Fig. 3a shows a plot of log of the zero shear viscosity enhancement, $\eta_0/\eta_{0,L}$, as reported by Costeux et al. [21], versus the average branch length, z_{br} . An exponential increase in the zero shear viscosity enhancement with increasing branch length is observed. The extrapolation of the fit intercepts the z_{br} axis around 4000 g/mole. This implies that the viscosity enhancement effect due to long-chain branching starts to occur, when the average branch length becomes about three times the entanglement molecular weight, M_e , of 1250 g/mole [12]. It has been previously reported that rheological properties are affected by branches of at least twice M_e [12].

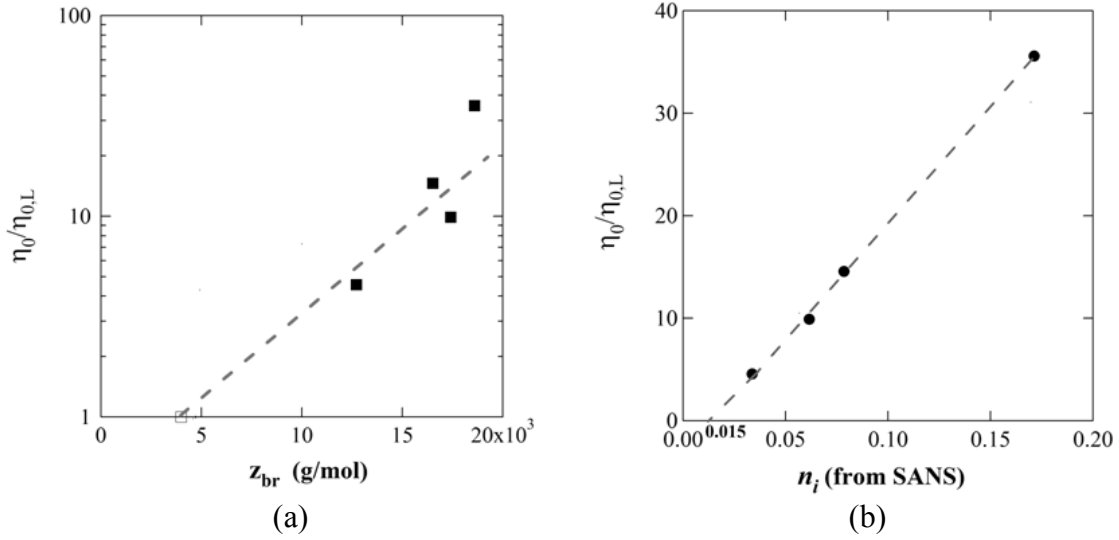


FIG. 3. (a) Log-linear plot of zero shear viscosity enhancement for linear polyethylene of same M_w [21] against average length of branch, z_{br} (from SANS), for the HDB samples. The extrapolation of z_{br} data intercepts the z_{br} axis at 4000 g/mole. (b) Linear plot of zero shear viscosity enhancement for linear polyethylene of same M_w [21] against number of inner segments per chain, n_i , for the HDB samples.

Based on previous studies [21, 23], the viscosity enhancement can also be attributed to the number of inner segments per chain, n_i , as described in Ref. [21], in branch-on-branch polymer chains. n_i can be approximated by $n_i = n_{br} - n_{br,p}$. Fig. 3b shows a plot of viscosity enhancement, $\eta_0/\eta_{0,L}$, versus n_i . The linear functionality of $\eta_0/\eta_{0,L}$ in n_i follows the Einstein approximation [24] for a particulate suspension, $\eta_0 = \eta_{0,L} (1 + n_i [\eta])$, except that there is a shift of about 0.015 in n_i . Einstein behavior indicates that chains containing inner segments do not contribute to flow, acting as particulate inclusions, and show a simple volumetric exclusion from the remaining viscous material composed of linear chains and non-hyperbranched chains. In the Einstein linear equation the slope, 228 chains/inner segment, corresponds to a type of intrinsic viscosity for hyperbranched-structures in a suspension of linear chains. The shift factor of 0.015 inner segments/chain may arise due to the presence of a small population (1 per 70 chains) of branches that are

not long enough to significantly affect viscosity, as described earlier. That is, some branches are seen as long chain by SANS but not by rheology since the definition of a long chain branch differs between the two methods.

A novel scaling approach to characterize long-chain branch content in polyethylene has been presented. Through this approach, the new quantities mole fraction branch content, ϕ_{br} , number of branch sites per chain, n_{br} , number of branch sites per minimum path, $n_{br,p}$, number of inner segments per chain, n_i , and average branch length, z_{br} , are reported. While ϕ_{br} quantifies the mole fraction long-chain branch content z_{br} can provide additional information about the architectural makeup of a polymer resulting in improved understanding of its rheological properties. $n_{br,p}$ when combined with n_{br} gives further details about the chain architecture. The approach encompasses both qualitative and quantitative analysis of long-chain branching in polyethylene. The scaling model has been successfully employed previously to determine branching in ceramic aggregates [3] and quantifying degree of folding in proteins and RNA [4]. This work further highlights the versatility of the model in studying complex nano- and macromolecular structures.

We thank L.J. Effler and A. W. deGroot of The Dow Chemical Company, for providing the polyethylene samples. This work utilized facilities supported in part by the National Science Foundation under Agreement No. DMR-0454672. We acknowledge the support of the National Institute of Standards and Technology (NIST), U.S. Department of Commerce, for providing the neutron research facilities. We thank Equistar Chemicals, LP for funding this work.

- [1] J. M. Desimone, *Science* **269**, 1060 (1995).
- [2] A. Arneodo, F. Argoul, E. Bacry, J. F. Muzy, and M. Tabard, *Physical Review Letters* **68**, 3456 (1992).
- [3] G. Beaucage, *Physical Review E* **70**, 10 (2004).
- [4] G. Beaucage, *Biophysical Journal* **95**, 503 (2008).
- [5] D. K. Bick, and T. C. B. McLeish, *Physical Review Letters* **76**, 2587 (1996).
- [6] D. J. Lohse, S. T. Milner, L. J. Fetters, M. Xenidou, N. Hadjichristidis, R. A. Mendelson, C. A. Garcia-Franco, and M. K. Lyon, *Macromolecules* **35**, 3066 (2002).
- [7] Z. B. Guan, P. M. Cotts, E. F. McCord, and S. J. McLain, *Science* **283**, 2059 (1999).
- [8] R. Everaers, S. K. Sukumaran, G. S. Grest, C. Svaneborg, A. Sivasubramanian, and K. Kremer, *Science* **303**, 823 (2004).
- [9] B. H. Zimm, and W. H. Stockmayer, *The Journal of Chemical Physics* **17**, 1301 (1949).
- [10] D. Yan, W. J. Wang, and S. Zhu, *Polymer* **40**, 1737 (1999).
- [11] P. M. Wood-Adams, and J. M. Dealy, *Macromolecules* **33**, 7481 (2000).
- [12] P. M. Wood-Adams, J. M. Dealy, A. W. deGroot, and O. D. Redwine, *Macromolecules* **33**, 7489 (2000).
- [13] A. S. Kulkarni, and G. Beaucage, *Journal of Polymer Science Part B-Polymer Physics* **44**, 1395 (2006).
- [14] W. Kuhn, *Kolloid-Zeitschrift* **68**, 2 (1934).
- [15] A. Guinier, and G. Fournet, *Small Angle Scattering of X-Rays* (Wiley, New York, 1955).
- [16] G. Beaucage, *Journal of Applied Crystallography* **28**, 717 (1995).
- [17] G. Beaucage, *Journal of Applied Crystallography* **29**, 134 (1996).
- [18] G. Beaucage, S. Rane, S. Sukumaran, M. M. Satkowski, L. A. Schechtman, and Y. Doi, *Macromolecules* **30**, 4158 (1997).
- [19] R. Ramachandran, G. Beaucage, A. Kulkarni, D. McFaddin, J. Merrick-Mack, and V. Galiatsatos, *Macromolecules* **41**, 9802 (2008).
- [20] C. M. Sorensen, and G. M. Wang, *Physical Review E* **60**, 7143 (1999).
- [21] S. Costeux, P. Wood-Adams, and D. Beigzadeh, *Macromolecules* **35**, 2514 (2002).
- [22] H. Murase, T. Kume, T. Hashimoto, Y. Ohta, and T. Mizukami, *Macromolecules* **28**, 7724 (1995).
- [23] D. J. Read, and T. C. B. McLeish, *Macromolecules* **34**, 1928 (2001).
- [24] A. Einstein, *Ann. Physik* **19**, 289 (1906).